Climatological Estimates of Lake Evaporation

F. I. MORTON

Hydrology Research Division, Environment Canada, Ottawa, Ontario K1A OE7

A model for estimating areal evaporation and transpiration is modified slightly to provide estimates of annual lake evaporation from monthly observations of temperature, humidity, and sunshine duration (or radiation) in the land environment. The model estimates tend to be higher than the more conventional estimates in humid areas and lower in arid areas, with the latter tendency particularly noticeable in the case of Lake Nasser on the Nile River. However, the results agree very well with comparable water budget estimates for Lake Hefner in Oklahoma, the Salton Sea and Silver Lake in California, Pyramid and Winnemucca lakes in Nevada, Lake Ontario on the border between New York and Ontario, and Dauphin Lake in Manitoba. They also compare reasonably well with energy budget estimates of the evaporation from Lake Mead on the border between Arizona and Nevada when the net inflow of heat is taken into account. A technique that provides such realistic results over a wide range of depths and environments with readily available data should prove very useful in water resource or environmental impact studies. Examples of such uses are provided by maps of Canada and the southeastern United States that show average annual values of the lake evaporation, and average annual values of the difference between the evaporation from a projected reservoir, and the combined evaporation and transpiration from the area before flooding.

INTRODUCTION

There is a wide gap between the kind of information that is needed for reliable estimates of lake evaporation and the kind of information that is available for estimating the lake evaporation input to water planning and management or environmental impact studies. Thus the former requires research on the scale of the International Field Year on the Great Lakes (IFYGL), the Lake Hefner studies, or the Salton Sea investigation, whereas the latter is limited to routine pan evaporation or climatological observations taken in a land environment. The gap is normally bridged by using the results of detailed research to develop coefficients that can be applied to pan evaporation or in the computation of potential evaporation from climatological observations.

There are several problems associated with this procedure. The first is that seasonal changes in subsurface heat storage are not reflected in pan or climatological observations, so that seasonal estimates of the evaporation from deep lakes are impractical. This limitation is not too important because annual estimates are adequate for most water planning and management or environmental impact studies. A much more serious problem is that pan and climatological observations are influenced by the land environment even if made on the shore of an existing lake. For example, it is widely recognized that the pan coefficients must be lower for lakes in arid regions than for lakes in humid regions. However, with the infinite variety of land environments and with little knowledge on how they influence the observations, there will always be considerable doubt about the transposability of coefficients or techniques from one lake to another.

A technique that is less sensitive to the contrasts between lake and land environments is presented herein. It is almost identical to an areal evaporation model [*Morton*, 1978] that provides estimates of the actual evaporation and transpiration from an area using routine observations of air temperature, dew point temperature, and sunshine duration. The results of this model have been tested successfully against comparable water budget estimates for 122 river basins in Canada, Ireland, Kenya, and the southeastern United States with no local optimization of coefficients. Changes to the albedo and the emissivity terms modify the model in such a way that it can provide estimates of monthly evaporation from shallow lakes and estimates of annual evaporation from any lake.

To test this capability, the model estimates have been compared with published water balance estimates for Lake Hefner in Oklahoma, Pyramid Lake and Winnemucca Lake in Nevada, Silver Lake and the Salton Sea in California, and Lake Ontario on the border between the Province of Ontario and the State of New York. These include a wide range of depths and land environments but do not include any lakes that have a lengthy period of ice cover. To remedy this situation, the model estimates have been compared with previously unpublished water balance estimates for Dauphin Lake in Manitoba. The good agreement between model and water budget estimates of lake evaporation over such a wide range of environments provides encouragement for the belief that the model is applicable anywhere in the world.

Similar comparisons have been made with energy budget estimates for Lake Mead on the Colorado River between Nevada and Arizona and with a synthesis of conventional pan and climatological estimates for Lake Nasser on the Nile River in Egypt and the Sudan. The model estimate of annual evaporation from Lake Mead is about 25% less than the energy budget estimate, although this difference can be reduced to about 11% if the net heat inflow to the lake is taken into account. In the case of Lake Nasser the difference between comparable estimates is much greater and exceeds 5% of the average Nile discharge. It is, of course, impossible to state with certainty which estimates are the most reliable. However, the good agreement between model and water budget estimates in similar environments suggests that the conventional pan and climatological approaches can give estimates that are much too high in arid regions.

The model has been used to prepare maps of average annual lake evaporation for the part of Canada to the east of the Pacific Divide and for the southern United States. Similar maps have been prepared for the difference between lake and areal evaporation to provide some idea of the effect of a large reservoir on the water balance. The formulation, verification, and discussion of the model and the four maps are presented herein.

Paper number 8W0815.
0043-1397/79/008W-0815$01.00

PHYSICAL CONSIDERATIONS

Potential evaporation has many definitions. The definition used herein is that potential evaporation is the evaporation estimated from climatological observations using

$$E_P = DR_W + (1 - D)f_W(v - v_D) \tag{1}$$

in which E_P is the potential evaporation, R_W is the net radiation if the surface were at air temperature, f_W is the vapor transfer coefficient; v and v_D are the saturation vapor pressures for air and dew point temperatures, respectively, $D = (1 + \lambda/\Delta)^{-1}$, Δ is the rate of change of saturation vapor pressure with respect to air temperature, λ is a heat transfer coefficient equal to $\gamma p + 4\epsilon\sigma(T + 273)^3/f_W$, γ is the psychrometric constant, p is the atmospheric pressure, σ is the Stefan-Boltzmann constant, ϵ is the surface emissivity, and T is the average of the maximum and minimum air temperatures.

Equation (1) was developed by *Kohler and Parmele* [1967] as a modification of the equation first formulated by *Penman* [1948]. The modification replaces γp by λ, thereby taking into account the effects of changes in surface temperature on net longwave radiation.

Areal evaporation is defined as the actual evaporation and transpiration from an area that is primarily land. Lake evaporation is defined as the evaporation from a water surface so large that the effects of the upwind shoreline transition can be ignored. It is considered to be the potential evaporation over the lake downwind of the shoreline transition.

According to (1) an increase in air temperature (as reflected in v) and a decrease in humidity (as reflected in v_D) would increase E_P. Following the cause-and-effect chain beyond the customary first link, it is found that such changes could be expected from the increase in heat flux and the decrease in vapor flux associated with a reduction in the availability of water for areal evaporation in the land environment. Interactions of this kind have provided the basis for the formulation of a complementary relationship between potential evaporation and areal evaporation and for the development of a model that provides estimates of areal evaporation from routine climatological observations [*Morton*, 1978]. They suggest that the potential evaporation will provide an estimate of lake evaporation that is too high if the temperature and humidity are observed in the land environment. The way in which potential evaporation changes in the transition from an arid to a humid environment can be illustrated by the results of dish evaporation observations in an irrigated area.

Davenport and Hudson [1967] measured the variation in evaporation across a series of irrigated and fallow fields in the Sudan Gezira using fiberglass dishes with black painted wells 11.3 cm in diameter and 3.6 cm in depth. The passage of air from the desert (or from the unirrigated fallow fields) over the irrigated cotton caused the dish evaporation above the cotton to decrease rapidly in the downwind direction and approach a low constant value within 300 m, the width of the fields. Furthermore, as the air passed from irrigated cotton across unirrigated fallow, the dish evaporation above the fallow increased rapidly in the downwind direction and approached but did not reach the value observed at the upwind edge of the irrigated area. Figure 1 shows the variation of dish evaporation across three irrigated fields on December 27, 1963. The ratio of daily dish evaporation at the downwind edges of irrigated cotton to that at the upwind edge of the irrigated area was 0.69 for the field with 'dry' soil, 0.60 for the field with 'moist' soil, and 0.53 for the field with 'wet' soil.

The decreases in dish evaporation across the cotton were associated with decreases in temperature and increases in humidity. The vapor pressures appeared to attain equilibrium values within the 300-m width of the fields, but the temperatures were still decreasing, possibly because the observations were made above the level of the crop and the dishes.

The dish evaporation for the wet field in Figure 1 shows what happens over a lake in an arid climate. Thus the upwind dish evaporation reflects the potential evaporation in the desert, and the low relatively constant dish evaporation near the downwind edge reflects the potential evaporation over most of the lake. Furthermore, the dish evaporation for the moist and dry fields provides an analogy for what happens over lakes in progressively more humid climates where the contrasts between lake and land environments are less extreme. Because the transition zone is so narrow, the lake evaporation would approximate the low constant downwind value of potential evaporation.

Priestley and Taylor [1972] have proposed an equation for estimating the evaporation from an area with saturated surfaces and no advection. Therefore it should apply to the evaporation from a body of water so large that the effects of the shoreline transition are negligible. When expressed in terms of lake evaporation E_W, the equation is

$$E_W = 1.26(1 + \gamma p/\Delta)^{-1}R_W \tag{2}$$

Equation (2) does not include the vapor pressure deficit, $v - v_D$ and thus avoids many of the difficulties associated with (1). However, it does have the following disadvantages:

1. It does not include a term for changes in subsurface heat storage and therefore is not applicable to estimating the evaporation from deep lakes for short periods of time.
2. It is consistent with the original equation for potential evaporation developed by *Penman* [1948], which does not take into account the effect of changes in surface temperature on net longwave radiation loss. Therefore it is not compatible with the use of (1) or with climatological estimates of net radiation.
3. It does not take into account the energy brought into the region by large-scale air mass movements during the fall and winter months when inversions of potential temperature extend to the surface for long periods of time.
4. The quantity Δ is a function of air temperature and therefore is significantly influenced by whether the observations are made in the land environment or in the lake environment.

Without records of subsurface temperature changes, there are limited prospects for reliable short-term estimates of the evaporation from deep lakes. All that can be done at the present time is to ignore the first disadvantage and hope for reliable estimates of annual evaporation. However, the latter three disadvantages can be overcome partially, at least, with

$$E_W = \psi(R_W + M) \tag{3}$$

in which the energy weighting factor ψ and the advection energy M are defined by

$$\psi = 0.26 + \left[1 + \frac{\lambda}{\Delta}\left(\frac{0.5 + 0.5r + \lambda/\Delta}{r + \lambda/\Delta}\right)\right]^{-1} \tag{4}$$

$$M = 0.66B - 0.44R_W \tag{5}$$

$$M \geq 0 \tag{6}$$

where r is the relative humidity, equal to v_D/v, and B is the net longwave radiation loss if the surface were at air temperature.

The derivation of (4) has been presented elsewhere [*Morton*, 1978]. Although based on a number of unverifiable assumptions, it provides a logical correction for the difference between the environment in which the temperature and humidity are observed and the environment that would exist if there were no limitations on the availability of water for evaporation. Its successful use in the areal evaporation model suggests that it would be even more useful in estimating lake evaporation.

The constants in (5) were determined by calibration of the areal evaporation model using climatological data from arid regions where the monthly areal evaporation could be assumed equal to the monthly precipitation [*Morton*, 1978]. Constraint (6) is an integral part of the relationship that eliminates the need for a complex function asymptotic to zero. It and all subsequent constraints function as "if" statements. For example, M is set equal to zero when (5) results in a value that is less than zero. This happens during the spring and summer months when R_W exceeds B by more than 50%.

Equations (3)–(6), inclusive, are used as the basis for a model that provides monthly estimates of net radiation and lake evaporation from any observations of air temperature, dew point temperature, and sunshine duration that are made in the vicinity of the lake. The modus operandi is outlined in the next section. As it is virtually identical to an areal evaporation model that has been published elsewhere [*Morton*, 1978], there is no need to complicate the presentation with detailed discussion of individual equations.

The complexity of the model is due to the use of sunshine duration to estimate the radiation components and to a generality that permits it to be used in any part of the world. Thus it can be simplified significantly if global radiation observations are available, if the monthly air temperatures never go below freezing, or if the lake is located between the tropics and the arctic or antarctic circles. However, simplification is rarely needed in this computer age. Both the areal evaporation and lake evaporation models are programed in Fortran and for the Hewlett Packard HP-67 pocket calculator. The documentation is available on request.

MODUS OPERANDI

For Each Lake

1. Assemble input:

φ latitude (negative in southern hemisphere), deg;
$\bar{P}$ long-term average annual precipitation, mm/yr;
p average atmospheric pressure, mbar;
H altitude above sea level, meters.

2. Compute the ratio of atmospheric pressure at the lake to that at sea level (p/p_s). If pressure observations are available, divide the average by 1013 mbar. If not, use the pressure correction equation for the standard atmosphere:

$$\frac{p}{p_s} = \left(\frac{288 - 0.0065H}{288}\right)^{5.256} \tag{7}$$

3. Estimate the minimum albedo for the land environment if the sun were at the zenith a_z:

$$a_z = 0.11 + 0.06 \exp\left(-\frac{\bar{P}}{920(p_s/p - \sin|\varphi|)}\right)^5 \tag{8}$$

4. Estimate the transmittancy of clouds to clear sky global radiation τ_c:

$$\tau_c = 0.28 + 0.10 \exp\left[-\left(\frac{\varphi}{38}\right)^8\right] - 0.04 \exp\left[-\left(\frac{\varphi}{6}\right)^8\right] \tag{9}$$

For Each Month

1. Assemble input:

T average of maximum and minimum air temperature, °C;
T_D average dew point temperature, °C;
S ratio of observed to maximum possible sunshine duration;
i month number beginning with 1 in January and ending with 12 in December;
n number of days in the month.

2. Compute the following:

$$v_D = 6.11 \exp\left(\frac{17.27\,T_D}{T_D + 237.3}\right) \tag{10}$$

$$v = 6.11 \exp\left(\frac{\alpha T}{T + \beta}\right) \tag{11}$$

$$\Delta = \frac{dv}{dT} = \frac{\alpha\beta v}{(T + \beta)^2} \tag{12}$$

in which α and β are 17.27° and 237.3°C, respectively, when T $\geq$ 0°C, or 21.88° and 265.5°C, respectively, when T $<$ 0°C.

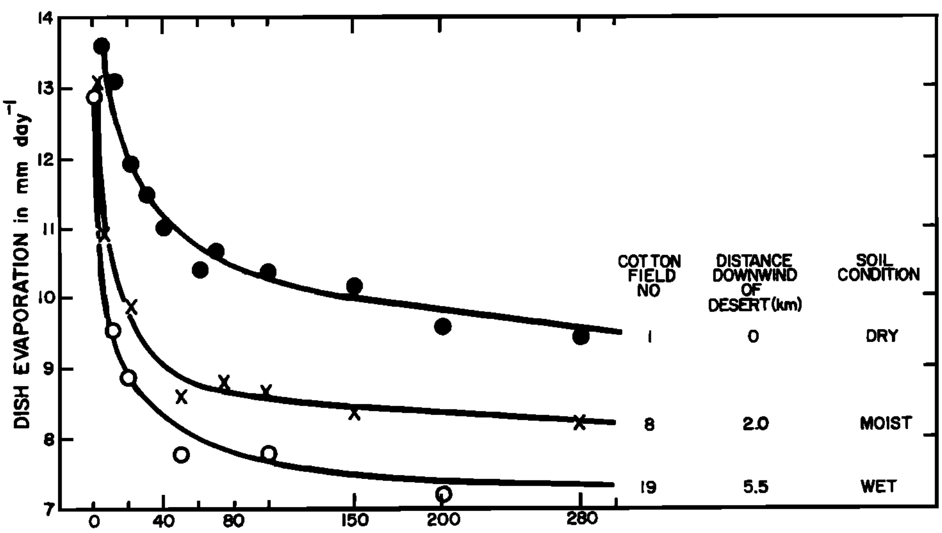

Fig. 1. Changes in dish evaporation across cotton fields on December 27, 1963.

3. Compute various angles and functions leading up to an estimate of the extra-atmospheric global radiation G_E:

$$\theta = 23.2 \sin (29.5i - 94) \quad (13)$$

$$\theta \geq \varphi - 89.999 \quad (14)$$

$$\theta \leq \varphi + 89.999 \quad (15)$$

$$\cos \omega = -\tan \varphi \tan \theta \quad (16)$$

$$\cos \omega \geq -1 \quad (17)$$

$$\cos z = \sin \varphi \sin \theta + \frac{180}{\omega \pi} \cos \varphi \cos \theta \sin \omega \quad (18)$$

$$\eta = 1 + \frac{1}{60} \sin (29.5i - 106) \quad (19)$$

$$G_E = (1354/\eta^2)(\omega/180) \cos z \quad (20)$$

in which θ is the declination of the sun, ω is the number of degrees the earth rotates between sunrise and noon, z is the average angular zenith distance of the sun, and η is the radius vector of the sun.

4. Compute the minimum albedo a_L and the maximum albedo a_U:

$$a_L = 0.04 [\exp (0.855) - ((1.71/\pi) \cos |\varphi - \theta| + \sin |\varphi - \theta|) \\ .\exp (0.0095 |\varphi - \theta|)]/[1.296 (1 - \sin |\varphi - \theta|)]^{-1} \quad (21)$$

$$a_U = a_L + (a_U - a_L) \quad (22)$$

in which $(a_U - a_L)$ is 0.00 when $T \geq 0°C$, and 0.60 when $T < 0°C$.

5. Compute various functions leading up to an estimate of the incident global radiation G:

$$W = \frac{v_D}{0.49 + T/129} \quad (23)$$

$$j = [0.47 + \cos^2 (\varphi - \theta)] \exp \left[84.2\left(\frac{p}{p_s} - 1\right)(0.17 - a_z)\right] \quad (24)$$

$$\tau = \exp \left[-0.089\left(\frac{p}{p_s \cos z}\right)^{0.75} - 0.083\left(\frac{j}{\cos z}\right)^{0.9} - 0.0288 \left(\frac{W}{\cos z}\right)^{0.6}\right] \quad (25)$$

$$\tau_a = \exp \left[-0.05 - 0.01\left(\frac{j}{\cos z}\right)^{1.8} - (0.00288)^{0.5}\left(\frac{W}{\cos z}\right)^{0.3}\right] \quad (26)$$

$$\tau_a \geq \exp \left[-0.05 - 0.01\left(\frac{j}{\cos z}\right)^{1.8} - 0.0288\left(\frac{W}{\cos z}\right)^{0.6}\right] \quad (27)$$

$$\tau_a \geq \tau \quad (28)$$

$$G_0 = G_E\tau \left[1 + \left(1 - \frac{\tau}{\tau_a}\right)(1 + a_z a_L \tau/0.04)\right] \quad (29)$$

$$G = G_0[\tau_c(1 - S) + S] \quad (30)$$

in which W is the precipitable water vapor, j is a turbidity coefficient, τ is the transmittancy of clear skies to direct beam solar radiation, τ_a is the part of τ that is the result of absorption, and G_0 is the clear sky global radiation.

6. Compute various quantities leading up to an estimate of the net longwave radiation loss B:

$$S^* = \frac{G/G_E - 0.18}{0.55} \quad (31)$$

$$0 \leq S^* \leq 1 \quad (32)$$

$$C = (1 - S^*)^{0.75} \quad (33)$$

$$\rho = 1 + [0.25 - 0.005 (v - v_D)]C^2 \quad (34)$$

$$\rho \geq 1 \quad (35)$$

$$B = \epsilon\sigma(T + 273)^4[1 - \rho(0.707 + v_D/158)] \quad (36)$$

in which S^* and C are the sunshine duration ratio and the cloud cover ratio estimated from global radiation, ρ is the ratio of average to clear sky atmospheric radiation, ϵ is the emissivity, and σ is the Stefan-Boltzmann constant. With ϵ assumed to be 0.97, $\epsilon\sigma$ is 5.50×10^{-8} W m^{-2} (°K)$^{-4}$.

7. Compute the minimum net radiation R_{WL}, the maximum net radiation R_{WU}, the stability factor ζ, the relative humidity r, the vapor transfer coefficient f_W, and the heat transfer coefficient λ:

$$R_{WL} = (1 - a_U)G - B \quad (37)$$

$$R_{WU} = (1 - a_L)G - B \quad (38)$$

$$\zeta = \left(\frac{|v - v_D|}{v_0}\right)^{0.12} \quad (39)$$

$$r = v_D/v \quad (40)$$

$$f_W = (\zeta f_W)/\zeta \quad (41)$$

$$\lambda = (\gamma p_s)\frac{p}{p_s} + \frac{4\epsilon\sigma(T + 273)^3}{f_W} \quad (42)$$

in which v_0 is the saturation vapor pressure at 0°C (6.11 mbar), ζf_W and γp_s are 22.0 W m^{-2} mbar^{-1} and 0.66 mbar °C^{-1}, respectively, when $T \geq 0°C$, or (22.0×1.15)W m^{-2} mbar^{-1} and $(0.66/1.15)$ mbar °C^{-1}, respectively, when $T < 0°C$.

8. Compute in the order shown,

$$D = \left(1 + \frac{\lambda}{\Delta}\right)^{-1} \quad (43)$$

$$\psi = \left[1 + \frac{\lambda}{\Delta}\left(\frac{0.5 + 0.5r + \lambda/\Delta}{r + \lambda/\Delta}\right)\right]^{-1} + 0.26 \quad (44)$$

$$M = 0.66B - 0.44R_{WU} \quad (45)$$

$$M \geq 0 \quad (46)$$

$$E = f_W(v - v_D) \quad (47)$$

$$E \geq \frac{0.7\psi}{1 - D} M + \frac{\psi - D}{1 - D} R_{WL} \quad (48)$$

$$M \leq \frac{(1 - D)}{\psi} E + \frac{\psi - D}{\psi} R_{WL} \quad (49)$$

$$R_W = R_{WU} \quad (50)$$

$$R_W \leq \frac{1 - D}{\psi - D} E - \frac{\psi}{\psi - D} M \quad (51)$$

$$E_P = DR_W + (1 - D)E \quad (52)$$

$$E_W = \psi(R_W + M) \quad (53)$$

TABLE 1. Evaporation From Lake Hefner and the Salton Sea in Millimeters

	Lake Hefner			Salton Sea			
				Model Estimate			
Month	Model Estimate	Water Budget Estimate	Year	With Sunshine Duration	With Radiation	Water Budget Estimate	Years Used in Average
January	50	63	1951	70	66	54	1961–1962
February	54	−16	1951	82	79	67	1961–1962
March	83	86	1951	123	112	99	1961–1962
April	124	69	1951	170	170	149	1961–1962
May	161	89	1951	204	217	216	1961–1962
June	182	149	1951	219	232	185	1961–1962
July	213	182	1951	230	242	215	1961–1962
August	194	224	1951	202	212	228	1961–1962
September	120	143	1950	153	154	218	1961–1962
October	98	165	1950	114	102	182	1961–1962
November	61	152	1950	76	73	118	1961–1962
December	47	72	1950	64	60	60	1961–1962
Annual	1387	1378		1707	1719	1791	

where E is defined in (47) and (48) and all other symbols have been defined previously.

9. Divide R_W, E_P, and E_W by the latent heat of vaporization (28.5 W-day/kg^{-1}) when $T \geq 0°C$, or by the latent heat of sublimation (28.5 × 1.15 W-day/kg^{-1}) when $T < 0°C$ and then multiply the number of days n to change W m^{-2} to kg m^{-2}. For water, this is equivalent to millimeters of depth.

Discussion

The only substantive differences between the lake and areal evaporation models are the use of 0.04 rather than a_z as the zenith value of minimum albedo in (21), the use of 0.00 rather than 0.05 as $a_U - a_L$ in (22) when the temperatures are at or above freezing, the use of 0.60 rather than 0.50 as $a_U - a_L$ in (22) when the temperatures are below freezing, and the use of 0.97 rather than 0.92 as the emissivity in (36). Equation (53), used to estimate lake evaporation, differs from the equation used to estimate areal evaporation, although it is an important component of the areal evaporation model.

Equation 52 is not essential to the computation of lake evaporation. However, it is useful for estimating the evaporation from ponds when edge effects such as those shown in Figure 1 are significant. The relative weights given to E_P, the evaporation at the upwind edge, and E_W, the evaporation downwind of the transition, in such an estimate are a matter of judgment but obviously depend on the average width of the pond in the direction of the prevailing winds.

Constraints (48), (49), and (51) prevent the computed lake evaporation from exceeding the computed potential evaporation. This would tend to occur during winter, when the most probable causes are the increase in albedo due to snow on the ice cover, overestimates of M due to uncertainties in the estimating procedure, and overestimates of v_D due to instrumental inadequacies. When R_W is constrained by (51) and used as input to (52) and (53), $E_W = E_P$ and $R_{WL} \leq R_W < R_{WU}$ (i.e., the albedo is greater than the minimum open water value and less than or equal to the maximum snow cover value). When M is constrained by (49) and used as input to (51), $E_W = E_P$ and $R_W = R_{WL}$. When E is constrained by (48) and used as input to (49), $E_W = E_P$, $R_W = R_{WL}$, and M is 70% of the original estimate. Thus constraint (51) is applied much more frequently than constraint (49), and constraint (49) is applied much more frequently than constraint (48).

When air temperatures are at or above freezing, the vapor pressure deficits $v - v_D$ are relatively high, so that it is most unlikely that constraints (48), (49), and (51) would apply. However, if they were to apply, there would be no difference in net radiation, since $a_U = a_L = 0.00$ and $R_{WL} = R_{WU} = R_W$. Therefore the only effect on the estimates of lake evaporation would be a reduction of up to 30% in the original estimate of the advection energy M, and this would normally be zero during the spring and summer.

The peculiar formulation represented by (31)–(33), inclusive, permits the model to be used with global radiation observations as input instead of sunshine duration observations. Under such circumstances, (8), (9), and (23)–(30), inclusive, become redundant. The model can also be modified to utilize both global and total hemispheric radiation observations by omitting (8), (9), (16)–(20), inclusive, and (23)–(35), inclusive, and by changing (36) to

$$B = \epsilon[\sigma(T + 273)^4 - A] \quad (54)$$

in which A is atmospheric radiation, the difference between total hemispheric and global radiation.

The model estimates of lake evaporation are most sensitive to errors in the sunshine duration or radiation observations. They are comparatively insensitive to errors in air temperature and dew point temperature, since the effects are limited to minor changes in the estimates of radiation, advection energy, and the energy weighting factor. Errors in the long-term average annual precipitation can influence the radiation estimates slightly by their effects on the zenith albedo for the land environment used in (24) and (29). Since (8) shows that a_z remains constant at 0.11 for the entire humid and subhumid range and at 0.17 for the entire arid range, it is only in the transition that precipitation errors can have any effect at all.

As mentioned earlier, the constants in (45) were derived by calibration of the areal evaporation model with climatological data from arid regions where the monthly areal evaporation could be assumed equal to the monthly precipitation [*Morton*, 1978]. The same calibration produced the value of ζf_W used in (41). Although the value for a lake may be somewhat different, the effects on the estimates of lake evaporation are limited to slight changes in the estimate of the heat transfer coefficient in (42) and to slight changes in the frequency of application of constraints (48), (49), and (51).

TABLE 2. Evaporation From Pyramid and Winnemucca Lakes in Millimeters

	Pyramid Lake			Winnemucca Lake		
Month	Model Estimate	Water Budget Estimate	Years Used in Average	Model Estimate	Water Budget Estimate	Years Used in Average
January	37	76	1935–1936	19	18	1937–1938
February	48	66	1935–1936	47	49	1936
March	86	67	1935–1936	79	68	1936–1938
April	121	78	1935–1936	120	113	1936–1938
May	168	44	1935–1936	171	155	1935–1937
June	187	79	1935–1936	188	223	1935–1937
July	198	143	1935–1936	198	204	1935–1937
August	172	148	1935–1936	176	203	1935–1937
September	123	130	1935–1936	123	105	1935–1937
October	84	155	1935–1936	85	63	1935–1937
November	51	139	1935–1936	50	42	1935–1937
December	34	150	1935–1936	34	26	1935–1936
Annual	1309	1275		1290	1269	

It should be noted that the discussion in the two preceding paragraphs refers only to estimates of lake evaporation. The potential evaporation estimates produced by (52) are much more sensitive to errors in air and dew point temperatures and in the calibrated value of ζf_W.

TEST PROCEDURE AND RESULTS

Water budget estimates of lake evaporation depend on the availability and reliability of precipitation, tributary inflow, groundwater inflow, outflow, and water level observations. This means that few lakes are suitable for water budget studies. For relatively small lakes the usual problem is the estimate of tributary inflow, as it is seldom completely measured and errors have a significant influence on the evaporation estimates. On large lakes the major problem can be the way the lakes themselves cause the precipitation to differ from that of the land environment. Despite these and other difficulties, the water budget remains the only convincing standard for judging the adequacy of lake evaporation models.

The model presented herein was formulated to provide estimates of monthly evaporation from shallow lakes and annual evaporation from deep lakes using observations of temperature, humidity, and sunshine duration (or radiation) in the land environment. These capabilities are tested by comparing the model estimates with published water budget estimates for Lake Hefner, the Salton Sea, Pyramid Lake, Winnemucca Lake, Silver Lake, and Lake Ontario. These six lakes provide a reasonably strict test, since they represent a wide range of depths and environments. However, the results of a previously unpublished water budget for Dauphin Lake have been added to extend the test range to lakes with a lengthy period of ice cover.

Lake Hefner is located in Oklahoma at 35°35'N and 97°40'W. It is approximately 365 m above sea level, has an average depth of almost 9 m, and an average area of almost 10.5 km². The climate is subhumid with an average annual precipitation near 790 mm. The water budget estimates of lake evaporation were an important part of the well-known Lake Hefner studies [*U.S. Geological Survey*, 1954]. The model estimates are based on the air temperature, dew point temperature, and sunshine duration observations at Oklahoma City. A comparison is presented in Table 1. The annual water budget estimate is 1378 mm, and the annual model estimate is 1387 mm, a difference of less than 1%. Similar figures for the year ending April 30, 1951, are 1343 and 1353 mm, respectively. The water budget evaporation tends to be lower than the model estimate during spring and early summer and higher during late summer and fall, as could be expected from the seasonal pattern of subsurface heat storage changes.

The Salton Sea is situated at 33°15'N and 115°50'W in the

TABLE 3. Evaporation From Silver Lake and Lake Ontario in Millimeters

	Silver Lake			Lake Ontario		
Month	Model Estimate	Water Budget Estimate	Year	Model Estimate	Water Budget Estimate	Year
January	65	60	1939	8	107	1973
February	71	119	1939	11	51	1973
March	128	145	1939	42	−5	1973
April	174	179	1939	75	10	1972
May	239	249	1938	121	43	1972
June	264	262	1938	121	41	1972
July	284	262	1938	159	38	1972
August	259	251	1938	122	66	1972
September	201	193	1938	76	89	1972
October	104	144	1938	42	127	1972
November	65	98	1938	21	97	1972
December	61	56	1938	5	66	1972
Annual	1915	2018		803	730	

TABLE 4. Evaporation From Dauphin Lake in Millimeters

Month	1967 Model Estimate	1967 Water Budget Estimate	1968 Model Estimate	1968 Water Budget Estimate	Average Model Estimate	Average Water Budget Estimate
January	−3	−5	−4	9	−3	2
February	−3	6	−1	−5	−2	1
March	4	34	37	23	20	28
April	34	78	76	25	55	52
May	110	93	104	96	107	94
June	132	126	121	107	126	116
July	157	150	152	154	154	152
August	136	55	98	129	117	92
September	78	105	65	83	72	94
October	29	58	33	49	31	54
November	8	5	6	−8	7	−1
December	−4	6	−3	7	−3	6
Annual	678	711	684	669	681	690

State of California. During 1961 and 1962 it was approximately 71 m below sea level, with an average depth near 8 m and an average area of about 910 km². The climate is arid with an average annual precipitation between 20 and 60 mm. The water balance estimates of evaporation and climatological observations at Sandy Beach have been published by *Hughes* [1967]. The climatological data are in graphical form, so that minor errors in abstraction are probable. Two different model estimates have been made, both based on the Sandy Beach air and dew point temperatures. They differ in that one uses Yuma sunshine duration observations to estimate radiation, whereas the other uses the Sandy Beach observations of global and total hemispheric radiation. The results shown in Table 1 permit comparison between the three different estimates. The average annual values agree very well, both model estimates being between 4 and 5% lower than the water budget estimates. The difference between the monthly estimates are not so clearly related to subsurface heat storage changes as those at Lake Hefner. As the depths are not significantly different, this is probably due to errors in computing the Salton Sea monthly water budget evaporation from values derived for shorter, irregular time periods.

It is interesting to note the close agreement between the average annual values for the two model estimates in view of the significant difference between the global radiation observed at Sandy Beach and the global radiation estimated from the Yuma sunshine duration. One explanation is that the global radiation observations are too low and the total hemispheric radiation observations are correct. Another is that the atmosphere at Sandy Beach is to some extent influenced by the Salton Sea, so that the global radiation is lower and the atmospheric radiation is higher than would be expected in an unmodified land environment.

Harding [1962] has published values of water budget evaporation for Pyramid and Winnemucca lakes in Nevada. They are located between 119°W and 120°W at a latitude of about 40°N and an elevation of about 1160 m above sea level. Pyramid Lake has an area of approximately 500 km² and an average depth exceeding 60 m. The depth and area of Winnemucca Lake were roughly 5 m and 60 km², respectively, in early 1935, but by late 1938 the lake was practically dry. The climate is arid with an average annual rainfall of approximately 165 mm. The model estimates computed from air temperatures, dew point temperatures, and sunshine duration recorded at Reno, Nevada, are compared with the water budget estimates in Table 2. The model estimates of average annual evaporation exceed the water budget estimates by less than 3% in the case of Pyramid Lake and less than 2% in the case of Winnemucca Lake. The differences between the monthly values of the water budget estimates for Pyramid and Winnemucca lakes clearly demonstrate the effects of depth on subsurface heat storage and the seasonal pattern of evaporation. It is interesting to note that the annual evaporation from Pyramid and Winnemucca lakes is less than that for Lake Hefner despite the sunnier and more arid climate.

Water budget estimates of the evaporation from Silver Lake in California have been published by *Blaney* [1957]. The lake is located at 35°25′N and 116°05′W at an altitude of approximately 280 m above sea level. In March 1938 the lake had an area exceeding 50 km² and a maximum depth of about 2 m, but by September 1939 most of the water in the lake had evaporated. The climate is arid with an annual rainfall of about 100 mm. Published values of air temperature and relative humidity for a station on the beach are available as input to the model but there are no sunshine duration or global radiation observations to be used as a basis for the radiation estimates. The lake is almost equidistant from Las Vegas, where later global radiation observations were high but within the expected range, and Inyokern (China Lake), where later global radiation observations were abnormally high. These later records indicate that there is little year-to-year variation in the global radiation in the vicinity of the lake. Therefore the radiation estimates in the model are based on the average monthly values of global radiation at Las Vegas for the 5 yr ending December 31, 1964.

Table 3 presents a comparison between the model estimates and the water budget estimates of the evaporation from Silver Lake. It shows that the annual model estimate is approximately 5% less than the annual water budget estimate and that the heat stored in less than 2 m of water has an insignificant effect on the seasonal pattern.

The evaporation from Lake Ontario has been estimated by the water budget technique for the IFYGL [*De Cooke and Witherspoon,* 1977]. The lake is centered at 43°39′N and 77°47′W at an elevation of 75 m above sea level. It has an area of 19,100 km² and an average depth of 86 m. During the IFYGL the precipitation on the lake, as estimated from the records of shoreline stations and radar, was 1025 mm, and

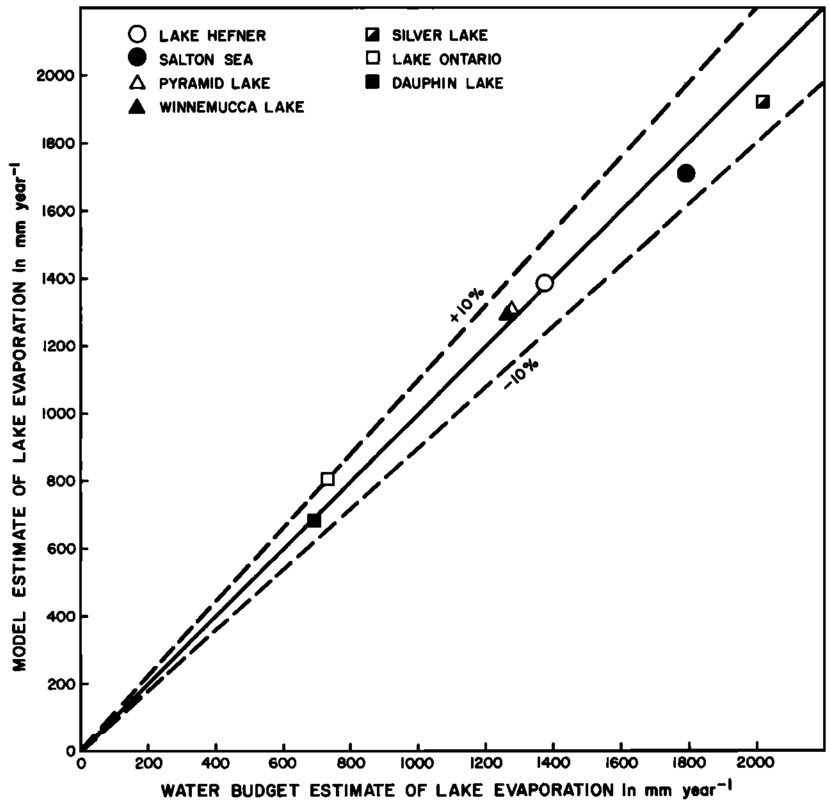

Fig. 2. Comparison of model and water budget estimates of lake evaporation.

monthly average shoreline air temperatures varied from 20°C in July to −8°C in February. Because of the great depth of the lake, the ice never covered more than half the area. The air and dew point temperature inputs to the model are averages of those recorded at Toronto International, Trenton, and Kingston airports, and the sunshine duration inputs are averages of those recorded at Kingston, Morven, Smithfield, Toronto, Hamilton, and Vineland. All of these stations are in Canada and may not be representative of the southeastern and eastern shores.

A comparison between the model estimates and the water budget estimates of the evaporation from Lake Ontario is presented in Table 3. It shows that the model estimate for the IFYGL is 10% higher than the water budget estimate. From examples provided by *De Cooke and Witherspoon* [1977] an error of this magnitude could be caused by an error in the outflows through the Saint Lawrence River of less than 0.6% or an error in the inflows from the Niagara River of less than 0.7%. The differences between the monthly model estimates and the monthly water budget estimates follow the general pattern expected from seasonal changes in subsurface heat storage in a very deep lake.

Dauphin Lake is located in the Province of Manitoba at 51°15'N and 99°46'W. It has an area of 521 km² and an elevation of 260 m above sea level. The average depth is not known but is believed to be less than 5 m. The average annual precipitation for the years 1967 and 1968 was between 390 and 400 mm. The lake was selected for the test because it has the characteristics and data needed for a reasonably successful water budget and because, unlike the other lakes, it has a long period of ice cover.

The Dauphin Lake water budget is for the years 1967 and 1968, the two driest consecutive years of record in the recent past. It is based on the records of outflow for the Mossy River, the records of water level at Ochre Beach and at the outlet, the records of precipitation at Dauphin Airport, and the records of tributary inflow for the furthest downstream gages on the Mink, Ochre, Turtle, Valley, Vermilion, and Wilson rivers. The gaged inflow is from an area of 5947 km² largely to the south and west of the lake. The ungaged inflow is from an area of 2468 km² concentrated on the east side of the lake and is estimated from the average of the unit runoffs for the four nearest gaged tributaries, i.e., the Mink, Valley, Ochre, and Turtle rivers. The resultant water budget estimates of the evaporation from Dauphin Lake are shown in Table 4.

In evaluating the water budget it should be noted that the estimated ungaged inflow is 36% of the estimated evaporation, that the gages on the tributary rivers do not operate during November, December, January, and February, when the flows are assumed to be insignificant, and that no attempt has been made to estimate groundwater inflows and outflows. On balance there is more chance that the water budget estimates of evaporation are too low than too high.

The model estimates of evaporation from Dauphin Lake are based on the records of air temperature, dew point temperature, and sunshine duration at Dauphin Airport. As can be seen from Table 4, the average annual value is 1.3% lower than the water budget estimate, and the difference in seasonal distributions is compatible with subsurface heat storage changes in a lake with a depth of 5 m.

Figure 2 provides a graphical comparison between the model and the water budget estimates of annual evaporation for the seven lakes. For such a wide range of environments the agreement is remarkably good. The average absolute deviation

TABLE 5. Evaporation From Lake Mead and Lake Nasser in Millimeters

	Lake Mead			Lake Nasser		
				Model Estimate		
Month	Model Estimate	Energy Budget Estimate	Year	With Sunshine Duration	With Radiation	Conventional Estimate
January	60	107	1953	103	103	121
February	73	129	1953	107	108	151
March	130	138	1953	139	138	229
April	163	138	1953	148	156	267
May	213	200	1952	179	179	310
June	238	304	1952	181	183	336
July	227	230	1952	177	175	332
August	216	278	1952	181	171	329
September	136	180	1952	146	149	285
October	108	134	1952	139	134	226
November	60	243	1952	113	110	189
December	50	143	1952	99	100	127
Annual	1674	2224		1712	1706	2902

from the line of equality is 47.6 mm y^{-1}, or 3.7%. The maximum deviations are 103 mm yr^{-1} and 10.0%.

Energy budget estimates of lake evaporation were made during the course of the well-known Lake Mead studies [*U.S. Geological Survey,* 1958]. The lake was formed by the construction of the Hoover Dam on the Colorado River between Arizona and Nevada at 36°01'N and 114°44'W. At the maximum controlled surface elevation of 372.3 m above sea level the lake area is 639 km^2 and the average depth is 57.5 m. The climate is arid with an average annual precipitation of less than 130 mm. The model estimates of evaporation from Lake Mead are based on the air and dew point temperature observations at Boulder City and the global and atmospheric radiation observations at Boulder Island, as recorded in the report on the Lake Mead studies. Table 5 provides a comparison between the model and the energy budget estimates for the 12-month period with the least change in subsurface heat storage during the 19-month period of study.

The model estimate of annual evaporation from Lake Mead is almost 25% less than the energy budget estimate. A significant part of this discrepancy is due to the net inflow of heat that can result when the inflows represent a large depth on the lake surface and have an average temperature much higher than the outflows. During the year ending April 30, 1953, the outflow from Lake Mead was equivalent to a depth of 34 m on the surface and the net inflow of heat was equivalent to 30.3 W m^{-2}, or 388 mm, of evaporation. The latter figure, when multiplied by the average annual value of the energy weighting factor (0.783) and added to the model estimate, gives a revised value of annual evaporation equal to 1978 mm, or 89% of the energy budget estimate.

With the specific heat of water equal to 4.19 J g^{-1} °C^{-1}, or 0.133 W-yr m^{-3} °C^{-1}, the figures in the preceding paragraph indicate that the average difference in temperature between the inflows and the outflows was $30.3/(34 \times 0.133)$, or 6.7°C. The latter value is of course a weighted average which takes into account the flow rates as well as the temperatures. When temperature differences and depth of inflow are of the same magnitude as those for Lake Mead, it is necessary to include an estimate of the net energy inflow as input to the model. This would occur normally only with deep reservoirs on large rivers in arid climates. The way in which the correction may be applied is illustrated below.

Lake Nasser was formed by the construction of the Aswan High Dam on the Nile River in Egypt at 23°55'N and 32°50'E. The lake floods back into the Sudan with a length of approximately 400 km and a maximum surface area of approximately 5000 km^2. The water surface elevation is about 180 m above sea level, and the maximum depth is about 95 m. The climate is arid with the average annual precipitation less than 30 mm. The evaporation has been estimated by *Omar and El-Bakry* [1970] using a synthesis of the conventional Dalton, Penman, McIlroy, and Class A evaporation pan approaches. Their results are compared with the model estimates in Table 5.

The model estimates are based on published monthly mean values of air temperature, dew point temperature, sunshine duration, and global radiation for Wadi Halfa in the Sudan near the south end of the lake [*Climates of Africa,* 1972]. The two versions whose results are presented in Table 5 differ in that one uses sunshine duration as input and the other uses global radiation as input. The differences between the two sets of model estimates are insignificant.

The model estimates are comparable to the conventional estimates, since neither takes into account the net inflow of heat or subsurface heat storage changes. The difference of 1200 mm/yr is equivalent to 6% of the average annual flow of the Nile River when the lake is near its maximum level. In evaluating the difference, it should be noted that the annual model estimates for Lake Nasser and the Salton Sea are almost identical and that those for the Salton Sea are only 4–5% less than the water budget estimate. Therefore there must be some significant difference between the environments of the two lakes, or there must be some flaw in the conventional ways of estimating evaporation when they are applied in a hot arid climate.

The average annual air temperature and estimates of global radiation are higher for Lake Nasser than for the Salton Sea. However, during the summer months, when both the evaporation and the difference between the two estimates are at their highest values, the temperatures are about the same, and the global radiation estimates are higher for the Salton Sea than for Lake Nasser. The somewhat lower humidities in the land environment around Lake Nasser could increase the evaporation within a few hundred meters of the upwind shoreline but could decrease the evaporation much more by their effects on the net longwave radiation loss over the entire lake. Therefore

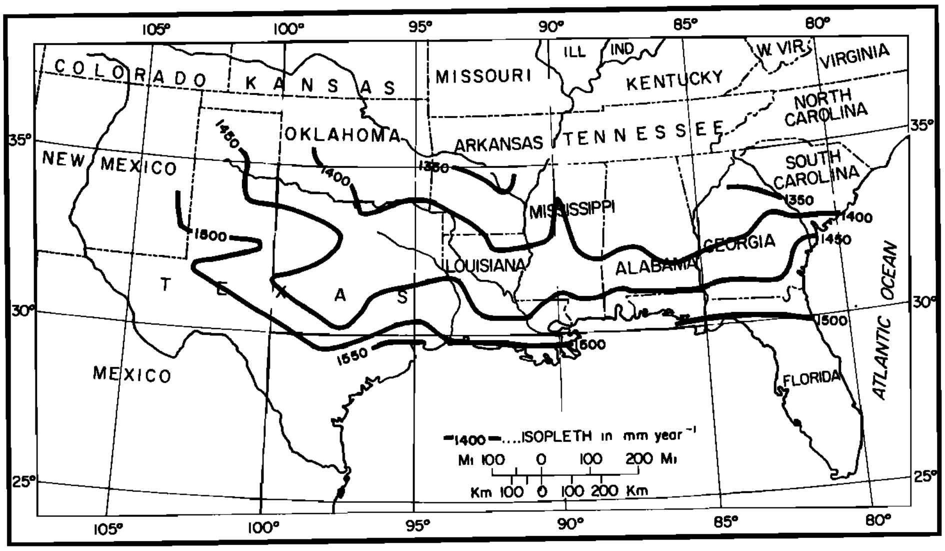

Fig. 3. Lake evaporation for 5 yr ending September 30, 1965.

it seems likely that the most important cause of the difference between the model and the conventional estimates of evaporation from Lake Nasser is the sensitivity of the conventional estimates to the vapor pressure deficits ($v - v_D$), which are much higher in the hot arid land environment where the input data originate than in the cooler, more humid lake environment.

In light of the foregoing considerations it seems probable that the model estimates of evaporation from Lake Nasser could be reasonably accurate. However, the characteristics of

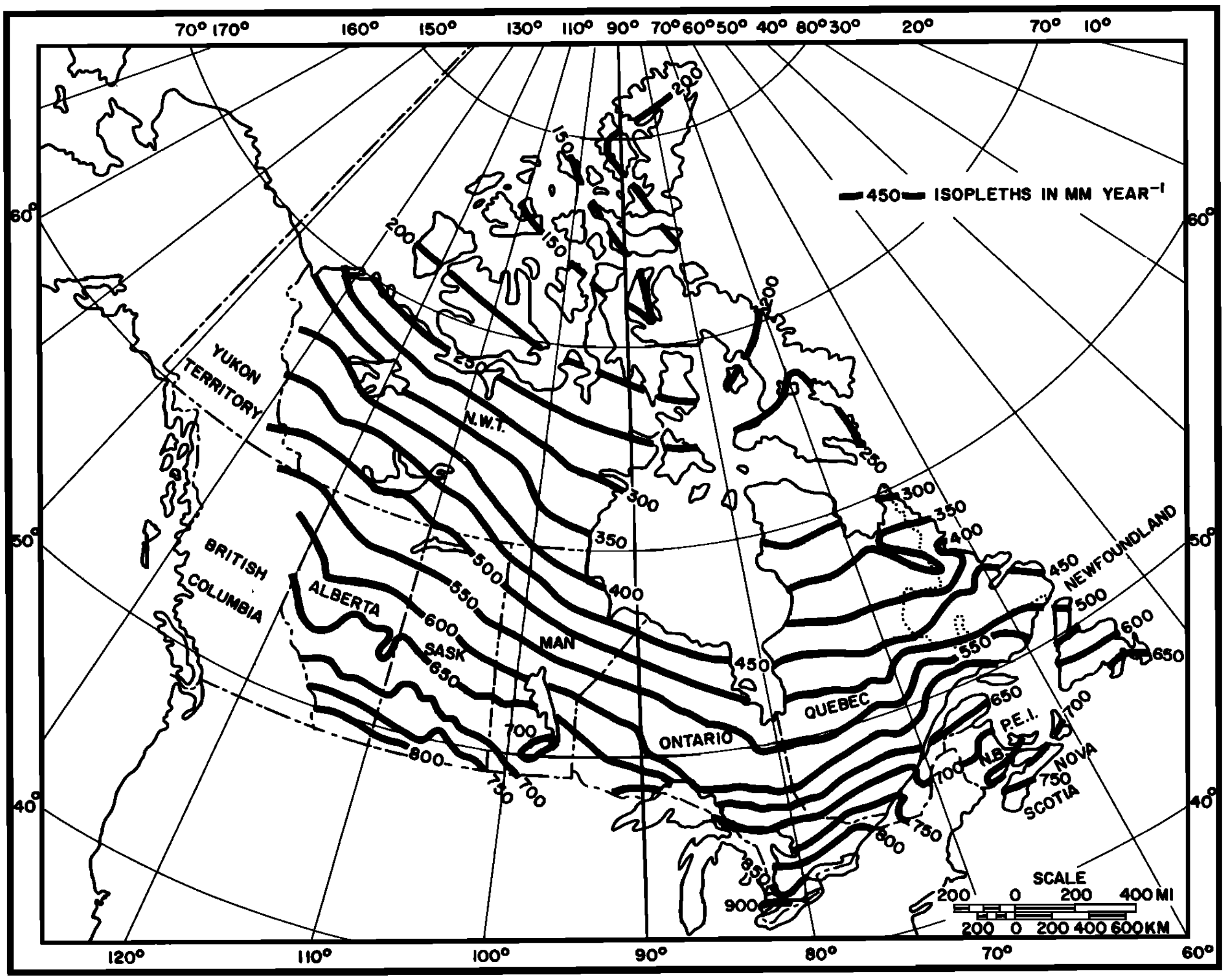

Fig. 4. Lake evaporation for 5 yr ending December 31, 1969.

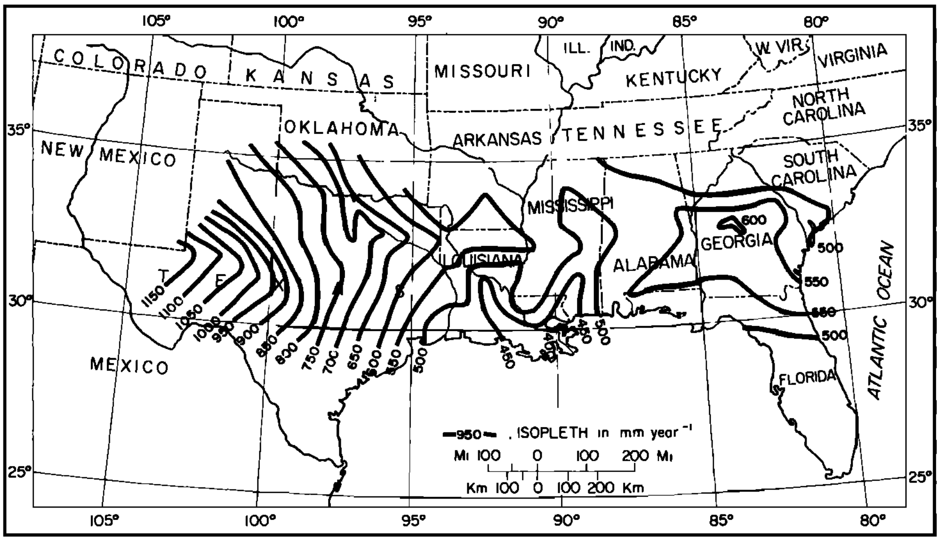

Fig. 5. Difference between lake and areal evaporation for 5 yr ending September 30, 1965.

the lake are such as to make the net inflow of heat a significant quantity. Thus the average flow of 2950 m^3 s^{-1} on an average area of 4500 km^2 represents a depth of 20.7 m yr^{-1}, and this, when multiplied by the average temperature difference between the Lake Mead inflows and outflows (6.7°C) and the specific heat of water (0.133 W-yr m^{-3} °C^{-1}), produces an average net inflow of heat equal to 18.4 W m^{-2}. Although it is reasonable to assume that the inflow of heat is high in the summer and negative in the winter, the way in which it becomes available for evaporation is not known. However, there should be little error in the annual estimate of evaporation if the average value is inserted in the enclosures of (53), along with the net radiation and advection energy, in the monthly computations. This would increase the model estimate of the evaporation from Lake Nasser to 1908 mm yr^{-1} if the sunshine duration is used, or 1902 mm yr^{-1} if the global radiation is used. These figures are still 1 m yr^{-1} less than the conventional estimates.

The discussion of Table 5 has demonstrated the need to include a term for the average net inflow of heat in the model when it is applied to deep lakes on large rivers in arid climates. With this adjustment the model estimates of evaporation from Lake Mead are in reasonable agreement with the energy budget estimates. However, the need for the adjustment cannot explain the large differences between the model estimates of evaporation from Lake Nasser and estimates based on a synthesis of the conventional Dalton, Penman, McIlroy, and Class A evaporation pan approaches. From the good agreement between the model and the water budget estimates of lake evaporation in comparable regions of North America it seems probable that the major cause of the differences is the sensitivity of the conventional estimates to the vapor pressure deficits ($v - v_D$), which are much higher in the hot, arid land environment where the input data originate than in the cooler, more humid lake environment. Therefore there is little evidence that the model, as adjusted to take into account the net inflow of heat, provides erroneous estimates of the evaporation from Lake Nasser.

SOME APPLICATIONS

The test of the areal evaporation model [*Morton*, 1978] required the preparation of evaporation maps for the part of Canada to the east of the Pacific Divide and for the southeastern United States. This involved punching computer cards with 5 yr of monthly air temperatures, dew point temperatures, and sunshine duration ratios for 37 climatological stations in the United States and 153 climatological stations in Canada. The availability of the cards provided the incentive to prepare similar maps for lake evaporation and for the difference between lake evaporation and areal evaporation.

Figure 3 is a map of the southeastern United States showing the average annual lake evaporation for the 5 yr ending September 30, 1965, and Figure 4 is a map of much of Canada showing the average annual lake evaporation for the 5 yr ending December 31, 1969. They are based on the accumulation of monthly model estimates for all climatological stations in the two areas that report both air and dew point temperatures. The isopleths were plotted by linear interpolation between the stations. It should be noted that the estimates shown in the two maps do not apply to bodies of water so small that the type of edge effect shown in Figure 1 would be significant or to lakes where there are large net inflows of heat.

A comparison of Figure 3 with a map published by *Miller et al.* [1963] and a comparison of Figure 4 with a map published by *Ferguson et al.* [1970] indicate that the model estimates are generally higher in areas with high relative humidities and lower in areas with low relative humidities. The reasons for these discrepancies are that all four maps are based on data from the land environment and that the model takes into account the differences between the land and the lake environments.

Figure 5 is a map of the southeastern United States showing the difference between the average annual lake evaporation and the average annual areal evaporation for the 5 yr ending September 30, 1965, and Figure 6 is a map of the part of Canada to the east of the Pacific Divide showing the difference between the average annual lake evaporation and the average annual areal evaporation for the 5 yr ending December 31, 1969. The lake evaporation estimates are those used to prepare Figures 3 and 4, and the areal evaporation estimates are those used in testing the areal evaporation model [*Morton*, 1978]. The isopleths were plotted by interpolation between the 190 climatological stations in the two areas that report both air and dew point temperatures.

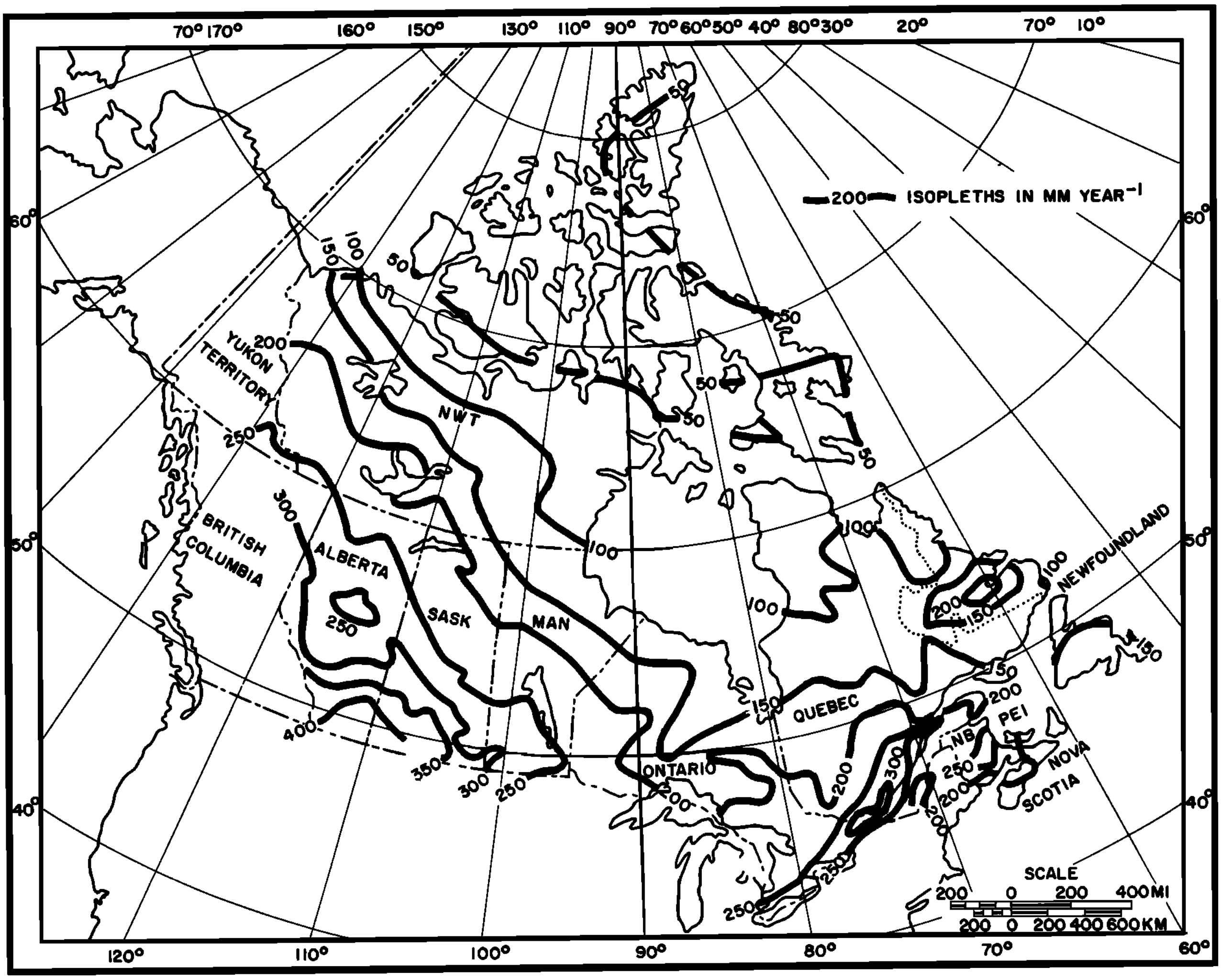

Fig. 6. Difference between lake and areal evaporation for 5 yr ending December 31, 1969.

The purpose of Figures 5 and 6 is to provide some indication of the effect on the water balance of constructing a reservoir when edge effects and net inflows of heat are insignificant. Such estimates are often needed for water resource or environmental impact investigations. The maps probably give values that are somewhat too high because the vegetation flooded by the reservoir would tend to transpire at a higher rate than the vegetation around the airports, where climatological stations are normally located.

SUMMARY

The model formulated herein permits estimates of annual lake evaporation to be made from routine climatological observations in the land environment. The input requirements are monthly averages of air temperature, dew point temperature, and sunshine duration. If the global radiation, the global and atmospheric radiation, or the global and total hemispheric radiation are available, they can be used as input instead of the sunshine duration, and if the average vapor pressure is available, it can be used as input instead of the dew point temperature. Also required are the latitude of the lake, the altitude (or average atmospheric pressure) for the lake, and a rough estimate of the average annual precipitation. If the inflows to the lake represent a large depth on the surface area and their average temperatures are significantly higher than the outflows, an estimate of the net inflow of heat is also needed.

Model estimates of annual lake evaporation are plotted against the comparable water budget estimates for Lake Hefner, the Salton Sea, Pyramid Lake, Winnemucca Lake, Silver Lake, Lake Ontario, and Dauphin Lake in Figure 2. These lakes represent a wide range of depths and environments, and the good agreement shown in Figure 2 provides a reasonable basis for the expectation that the model will give realistic estimates elsewhere. This expectation is strengthened by the relatively good agreement between the model and the energy budget estimates of the evaporation from Lake Mead when the net inflow of heat is taken into account.

The model estimates of evaporation from Lake Nasser are much lower than estimates based on a synthesis of the conventional Dalton, Penman, McIlroy, and Class A evaporation pan approaches. The difference is highly significant, since it represents 5–6% of the average annual flow of the Nile River. With the confidence engendered by the successful test of the model in similar environments elsewhere, it is reasonable to conclude that the conventional approaches produce erroneous results in hot, arid climates when they depend on climatological and pan observations in the land environment.

The capability of the model to produce quick and realistic estimates of annual lake evaporation from climatological ob-

servations in the land environment should prove very useful in water resource or environmental assessment investigations. The only problem in producing maps such as those shown in Figures 3 and 4 is in assembling the required input data. The usefulness can be enhanced further by combining the results with the results of the previously published areal evaporation model [*Morton*, 1978]. Thus maps like Figures 5 and 6, which show the difference between the lake and the areal evaporation, can provide an estimate of the effect on the water balance of constructing a reservoir.

NOTATION

The symbols used in this paper are defined below. Note that radiation and advection energy are expressed in terms of average power and evaporation is expressed in terms of average power consumption.

a_L minimum albedo.
a_U maximum albedo.
a_z minimum albedo of land environment if the sun were at the zenith.
A atmospheric radiation, W m^{-2}.
B net longwave radiation loss if the surface were at air temperature, W m^{-2}.
C cloud cover ratio estimated from global radiation.
$D = (1 + \lambda/\Delta)^{-1}$.
$E = f_W(v - v_D)$, W m^{-2}.
E_W lake evaporation, W m^{-2}.
E_P potential evaporation, W m^{-2}.
f_W vapor transfer coefficient, W m^{-2} mbar^{-1}.
G incident global radiation, W m^{-2}.
G_E extra-atmospheric global radiation, W m^{-2}.
G_0 clear sky global radiation, W m^{-2}.
H altitude above sea level, meters.
i month number.
j turbidity coefficient.
M advection energy, W m^{-2}.
n number of days in month.
p average atmospheric pressure at altitude H, mbar.
p_s average atmospheric pressure at sea level, mbar.
$\bar{P}$ long-term average annual precipitation, mm yr^{-1}.
r relative humidity, equal to v_D/v.
R_W net radiation if the surface were at air temperature, W m^{-2}.
R_{WL} minimum value of R_W.
R_{WU} maximum value of R_W.
S ratio of observed to maximum possible sunshine duration.
S^* sunshine duration ratio estimated from global radiation.
T average of maximum and minimum air temperature, °C.
T_D average dew point temperature, °C.
v saturation vapor pressure at T, mbar.
v_D saturation vapor pressure at T_D, mbar.
v_0 saturation vapor pressure at 0°C, mbar.
W precipitable water vapor, millimeters.
z average angular zenith distance of sun, deg.
α coefficient used in estimating vapor pressures.
β coefficient used in estimating vapor pressures, °C.
γ psychrometric constant, °C^{-1}.
Δ rate of change of saturation vapor pressure with respect to air temperature (dv/dT), mbar °C^{-1}.
ϵ surface emissivity.
ζ stability factor.
η radius vector of sun.
θ declination of sun, deg.
λ heat transfer coefficient, mbar °C^{-1}.
ρ ratio of average to clear sky atmospheric radiation.
σ Stefan-Boltzmann constant, W m^{-2} (°K)$^{-4}$.
τ transmittancy of clear skies to direct beam solar radiation.
τ_a the part of τ that is the result of absorption.
τ_c transmittancy of clouds to clear sky global radiation.
φ latitude (negative in southern hemisphere), deg.
ψ energy weighting factor.
ω number of degrees the earth rotates between sunrise and noon.

Acknowledgments. Unless otherwise acknowledged, the climatological and hydrological data used to test the model were published by the Atmospheric Environment Service of Canada, the Water Survey of Canada, and the U.S. Department of Commerce.

REFERENCES

Blaney, H. F., Evaporation study at Silver Lake in the Mojave Desert, California, *Eos Trans. AGU, 38*(2), 209–215, 1957.
Climates of Africa, World Survey of Climatology, vol. 13, p. 122, Elsevier, New York, 1972.
Davenport, D. C., and J. P. Hudson, Changes in evaporation rates along a 17-km transect in the Sudan Gezira, *Agr. Meteorol., 4*(5), 339–352, 1967.
De Cooke, B. G., and D. F. Witherspoon, International Field Year for the Great Lakes scientific report of the terrestrial water balance panel, IFYGL Steering Comm., Ann Arbor, Mich., 1977.
Ferguson, H. L., A. D. J. O'Neill, and H. F. Cork, Mean evaporation over Canada, *Water Resour. Res., 6*(6), 1618–1633, 1970.
Harding, S. T., Evaporation from Pyramid and Winnemucca lakes, Nevada, *J. Irrig. and Drain. Div. Amer. Soc. Civil Eng., 88*(IR1), 1–13, 1962.
Hughes, G. H., Analysis of techniques used to measure evaporation from Salton Sea, California, *Prof. Pap. 272-H*, U.S. Geol. Surv., Washington, D. C., 1967.
Kohler, M. A., and L. H. Parmele, Generalized estimates of freewater evaporation, *Water Resour. Res., 3*(4), 997–1005, 1967.
Miller, D. W., J. J. Geraghty, and R. S. Collins, Water atlas of the United States, plate 18, Water Inform. Center, Port Washington, New York, 1963.
Morton, F. I., Estimating evapotranspiration from potential evaporation: Practicality of an iconoclastic approach, *J. Hydrol., 38*, 1–32, 1978.
Omar, M. H., and M. M. El-Bakry, Estimation of evaporation from Lake Nasser, *Meteorol. Res. Bull., 2*(1), 1–27, 1970.
Penman, H. L., Natural evaporation from open water, bare soil and grass, *Proc. Roy. Soc. Ser. A, 193*, 120–145, 1948.
Priestley, C. H. B., and R. J. Taylor, On the assessment of the surface heat flux and evaporation using large-scale parameters, *Mon. Weather Rev., 100*, 81–92, 1972.
U.S. Geological Survey, Water-loss investigations, Lake Hefner studies, *Prof. Pap. 269*, Washington, D. C., 1954.
U.S. Geological Survey, Water-loss investigations, Lake Mead studies, *Prof. Pap. 298*, Washington, D. C., 1958.

(Received February 22, 1978;
revised May 18, 1978;
accepted July 27, 1978.)